

TRANSCRIPTOME PROFILING OF POTASSIUM STARVATION RESPONSIVENESS IN FLAX (*LINUM USITATISSIMUM* L.)

WENGONG HUANG^{1,2}, SHUQUAN ZHANG², GUANGWEN WU², YING YU², CHUANYING REN³, QINGHUA KANG^{2*}, YAN LIU², CHUNBO LIANG², LIGUO ZHANG² AND YAGUANG ZHAN^{1*}

¹College of Life Science, Northeast Forestry University, Harbin 150040, China

²Institute of Industrial Crops, Heilongjiang Academy of Agricultural Sciences, Harbin 150086, China

³Food Processing Institute, Heilongjiang Academy of Agricultural Sciences, Harbin 150086, China

*Corresponding authors e-mail: zhanyaguang2002@163.com; kang_qinghua@126.com; Tel: +86 0451 86677430

Abstract

Potassium (K) is an essential plant nutrient. The significance of potassium can be appreciated by observing plants grown under K⁺-deficient conditions, which greatly restricts growth and development and results in loss of crop quality and yield. Flax (*Linum usitatissimum* L.) is a significant economic crop that is often negatively impacted by K⁺ deficiency. To highlight K⁺ deficiency response mechanisms and increase flax potassium absorption and utilization ratio, flax variety Sofie was studied by studying seedlings after growing with or without K⁺ supply for 12h and 96h. cDNA was sequenced using an Illumina system. Genes involved in different regulatory mechanisms of K⁺-uptake during 12h and 96h stress were identified. In the K⁺-starvation group, 1154 and 247 differentially expressed genes (DEGs) were discovered after 12h and 96h of starvation, respectively. The results showed that 546 DEGs were annotated to 46 transcription factor families, 262 DEGs were annotated to signal transduction proteins or as participants in signal transduction pathways, 102 DEGs were annotated to hormone response proteins and 106 DEGs were annotated to transporter proteins. Multiple ion channels were also identified among the DEGs, including ion channel proteins homologous to AKT channels, KAT channels and CNG ion channels. This is the first study to analyze molecular response mechanisms of the flax transcriptome in response to K⁺ deficiency. These data provide numerous candidate genes with K⁺ deficiency that should guide future studies to elucidate plant strategies for adaptation to potassium deficiency.

Key words: Flax; Potassium deficiency; RNA-seq; Differentially expressed genes.

Introduction

Worldwide, potassium deficiency is very common. In China, 12.5% of the total area of cultivated soil exhibits either potassium deficiency or extreme deficiency that greatly limits normal crop growth and development. China's potassium resources are inadequate and dependent on importation of this nutrient, the area of potassium deficiency in cultivated soil is actually increasing (Gao *et al.*, 2000). With the development of modern agriculture, the increasing discrepancy of potassium fertilizer supply and demand has become a great concern. Meanwhile, previous studies have shown that various species and even different varieties within a crop species exhibit significant differences in soil potassium utilization (Liu & Liu., 2002). Recently, modern biological methods, such as transgene methodologies and molecular cloning, have been used to improve both potassium uptake and utilization efficiency (Wang *et al.*, 2010b). These measures should ultimately alleviate further depletion potassium deficient resources and improve crop yield and quality.

Potassium uptake utilization efficiency and potassium resistance are important measures of crop fertilizer utilization. Scholars from across the world have conducted much research on rice (Liu & Liu, 2002; Yang *et al.*, 2003), wheat (Yang *et al.*, 1998), cotton (Tian *et al.*, 2008), barley (Wu *et al.*, 2011) and flax. Such studies have demonstrated that potassium application can improve flax fiber quality, flax fiber rate, strength and lodging resistance (Zhao *et al.*, 1991), as well as increase both the yield of flax fiber and long fiber rate. The mechanism by which potassium exerts these positive effects is thought to operate through increasing the

photosynthesis and enzyme activities, but additional studies are needed to understand the specific mechanisms responsible for these effects (Li *et al.*, 1998).

Potassium, which constitutes 2%~10% of the total amount of plant dry matter and is the most abundant positive ion in plants, plays an important role in growth and development. More specifically, K⁺ participates in multiple enzymatic reactions in plant cells, including pyruvate kinase, fructose phosphate kinase, glutathione synthetase, starch synthase and malic acid synthetase. Consequently, K⁺ deficiency negatively affects plant metabolism through disruption of enzyme activities, especially since potassium is an activator of various enzymes (Pettigrew, 2008). Due to K⁺ concentration variations in soils, plants have evolved two types of potassium ion transport systems with distinct K⁺ affinities: one of low affinity for potassium and the other of high affinity (Epstein *et al.*, 1963). Because potassium ion transport is crucial for plant growth in potassium-deficient soils, it is not surprising that numerous potassium channels have been discovered, such as the KT/KUP/HAK transporter family (Rubio *et al.*, 2010; Bañuelos *et al.*, 2002; Wang *et al.*, 2002) and the KCOs family (Voelker *et al.*, 2006). Other transporters with dual functions have also been discovered, including the HKT transporter, with a dual function of Na⁺ and K⁺ transport (Munns & Tester, 2008) and CBL-CIPK, which is regulated by a Ca²⁺ signal pathway and which activates the AKT1 channel (Xu *et al.*, 2006; Lan *et al.*, 2011; Mao *et al.*, 2016). In addition, RCI3/RAP in the ROS signaling pathway is known to activate the transporter HAK. If plants lack potassium, they will show obvious symptoms: weak stems, easy lodging, water loss from leaves, reduction of both drought tolerance and cold resistance, decomposition

of protein and chlorophyll, yellowing of leaves and eventual signs of tissue necrosis (Munson, 1985). Ultimately, potassium deficiency in cultivated soil directly leads to a significant decline in crop yield and quality.

Due to recent advances that have increased genomic sequences with lots of plant species, low potassium stress transcriptome of several field crops and important economic plants have been studied, such as rice (Zhang *et al.*, 2017; Ma *et al.*, 2012), wheat (Ruan *et al.*, 2015), barley (Zeng *et al.*, 2014), watermelon (Fan *et al.*, 2014), tobacco (Lu *et al.*, 2015), sugarcane (Zeng *et al.*, 2015) and pear (Shen *et al.*, 2017). However, no such research on flax has yet been reported. Therefore, this study has great significance for successful cultivation of flax to potassium resistance. In addition, our results should provide a foundation of knowledge to guide research of other important economic plants and crops. Flax is a widely cultivated crop with an ancient history. This crop has great economic value as the main source of fiber, in addition to its extensive food and medicinal value. Recent publication of the flax genome sequence map (Wang *et al.*, 2012) has greatly facilitated flax research and has suggested existence of a low potassium response mechanism involving an activator protein. However, at the present time the growth and developmental response mechanism to potassium stress and the genes and ion channels participating in this regulatory process are all still unknown.

This study describes transcriptome sequencing of flax seedlings grown under conditions of varying potassium ion concentrations, from short-term to long-term stress exposure. As a result of this work, numerous DEGs and several significant pathways with potassium deficiency have been identified and lots of genes and several pathways for flax reaction to short-term and long-term low potassium stress are discussed. From this study, a foundation of our results will guide future genetic strategies to improve potassium tolerance in plants.

Materials and Methods

Flax materials and culture environment: Flax variety Sofie was adopted in this study. Sofie was granted by HAAS. Sofie seeds were planted in paper cups with sterilized vermiculite. Sofie seedlings were grown into artificial climate box 22°C for 16-h light/8-h dark and 70% RH. Irrigating with 1/2 Murashige and Skoog medium every 3 days.

Experiment treatments and plants operation: 3 weeks seedlings were turned into bottles of filled with nutrient solution containing an ample supply of K⁺ (ck) or treated solution without potassium (without potassium chloride) by potassium starvation treatment (ks). For the ck nutrient solution, modified Murashige and Skoog medium that containing KCl substituted for KNO₃ was used. This test was repeated thrice. There were 10 flax seedlings in each bottle during potassium stress treatment. 200 milliliters of nutrient solution were irrigated per bottle per time. After exposing ck and ks seedling to treated solution with 12h and 96h, plants were placed in a refrigerator with -80°C in

order to use for RNA extracting. The control group was the same as the operation above. Each control or experimental sample consisted of more than ten seedlings.

RNA-sequencing process: Total RNA was extracted by TRIzol and isolated from four groups of 3 repetitions each and included Sofie control (ck) and experimental samples (ks) grown for 12h and 96h and designated 12h-ck-1, 12h-ck-2, 12h-ck-3, 12h-ks-1, 12h-ks-2, 12h-ks-3, 96h-ck-1, 96h-ck-2, 96h-ck-3, 96h-ks-1, 96h-ks-2 and 96h-ks-3.

After total RNA isolation, remaining DNA was digested with DNase I, and RNA quality and quantity analyses were conducted. Isolating mRNA of poly-A was by Oligo dT. cDNAs were synthesized by mixing mRNA with fragmentation buffer. Purifying short cDNA fragment, then used EB for ends repairing and single nucleotide A (adenine) addition. Small fragment was connected to adapter, right parts were subjected to PCR reaction. Quantification and qualification of each sample library were tested by Agilent 2100 Bioanalyzer and ABI StepOnePlus Real-time PCR System. Finally, the libraries were sequenced by Illumina HiSeq 4000 System.

Transcript data analysis: After the accomplishment of sequence, raw reads were obtained and in-house software for obtaining clean reads. Reads containing low-quality were raw reads, adaptor-predominant reads and reads with a high content of unknown bases (N). Such noisy reads were eliminated before downstream analysis was performed. These reads were filtered. We define low quality read as one with a percentage of bases with quality of less than 10 or more than 20% for the reads. "Clean Reads" were remaining reads and stored in FASTQ (Cock *et al.*, 2010) format.

Next, clean reads were mapped to transcripts and flax reference genome by TopHat2 (Kim *et al.*, 2013) transcripts sequence alignment software. TopHat2 can support segmentation alignment independent of reference gene annotation, which facilitates discovery of a greater number of novel transcripts. Sequence alignment engine Bowtie2 (Langmead *et al.*, 2012) intercepted reads which could not be matched to small segments and inferred the location of these read segments. For reads originally unmatched, TopHat2 built a splice site reference set without relying on known genetic annotations. The alignment of RNA-Seq sequences not only helped to detect variable splicing and new transcripts, but also could be used to identify gene expression levels by recording transcript quantity. Alignment of mRNA-derived sequences to the genome only detects exonic genomic sequences and use of the StringTie tool (Pertea *et al.*, 2015) identified exon regions to help achieve reconstitution of transcripts. This software is based on a network flow algorithm derived using optimization theory in combination with de novo assembly. Finally, all assembled transcript fragments were aligned to reference genes and merged. After novel transcripts were identified, coding transcripts originating from them were amalgamated into reference transcripts for gaining a complete reference sequence library.

Next, gene expression analysis was performed by mapping transcripts against the reference sequence library. Gene expression levels were calculated using RSEM (Li & Dewey, 2011). Using mapping result, reads coverage and reads distribution of transcripts were calculated. In order to determine read counts aligned against each transcript for each sample to eliminate the influence of the sequencing amount and gene length, transcript per million (TPM) values were used to estimate gene expression levels. For measuring different expression levels of genes with respective treatments, TPM calculation method is more suitable than RPKM or FPKM. At the same time, in order to screen for actual expressed transcripts and eliminate false positive results, transcripts of low expression level were filtered using a TPM filter setting of TPM > 0.5 for at least one transcript per sample.

DEGs were detected using the software R package (Anders *et al.*, 2013). DEGs were filtered using a cutoff parameter of a differential fold difference of ≥ 2.00 and a q value ≤ 0.05 . DEGs responding to K^+ deficiency were screened using the threshold of q -value.

Next, DEGs were detected and further functional enrichment analysis was performed for all samples. DEGs were mapped to each functional category with GO database and numerous genes belonging to every category was computed to generate the genes lists and gene count for a given GO function. Next, the hyper geometric test was applied to determine the GO functional items for which DEGs were significantly enriched by comparing the results against those for the entire genome background. The p -value (cutoff=0.05) for KEGG annotation after functional enrichment of DEGs was also performed in the same way as was done for GO analysis. DEGs were blasted to Plant TFDB 3.0 (Jin *et al.*, 2014) to identify TFs.

$$P = 1 - \sum_{i=0}^{m-1} \frac{\binom{M}{i} \binom{N-M}{n-i}}{\binom{N}{n}}$$

Quantitative RT-PCR analysis: For qPCR analyses was performed to validate DEGs sequence results. First-strand cDNA was synthesized by 1 μ g of total RNA with oligo (dT) by M-MLV reverse transcriptase in accordance with commodity instruction. PCR was conducted by ABI7500 Real-time PCR System and SYBR Premix Ex Taq™ in accordance with commodity instruction. qPCR reaction was as follows: 95°C 30s, then 45 cycles of 95°C 5s, 60°C 40s, and 72°C 10s. The melting curve was determined after 45 cycles for verifying primers specificity. Quantitative PCR experiment was conducted by 3 biological repetitions. The flax actin gene was conducted for an internal reference with quantitative PCR analysis. The relative expression of gene was calculated by $2^{-\Delta\Delta Ct}$. This experiment, primer was devised by Primer 3.

Results

Analysis of RNA sequencing data: For each flax seedling sample subjected to K^+ starvation for 12h or 96h and corresponding unstressed controls, approximately 38.07 million raw reads were obtained by RNA-Seq, of which 95.38% were clean reads. Mapping them to the flax genomic sequence was conducted and demonstrated that at least 86.17% of reads successfully matched the reference genome sequence (Table 1).

To verify the results of RNA sequencing 8 genes were selected for qRT-PCR (Additional file 1: Table S1). The decision coefficient r^2 of gene expression variation data reached 0.91 for these two methods; therefore, the sequencing data met the accuracy requirement and could be used for the next analysis (Fig. 1).

Analysis of DEGs: After K^+ starvation for 12h, 1154 K^+ starvation response expression genes were identified. After 96h of potassium starvation, the number of DEGs was significantly reduced and 247 DEGs were identified.

Table 2 shows the top10 DEGs exhibiting up- and down-regulated expression for both stress-duration periods. An integrated analysis of all DEG annotation results showed that enzymes and HSPs dominated the top10 list. Furthermore, the difference in expression of HSPs between the 12h-ck vs 12h-ks samples was greater than between 96h-ck vs 96h-ks samples.

Table 1. Major characteristics of twelve libraries.

Sample	Total raw reads (M)	Total clean reads (b)	Mapped reads		Uniquely mapped	Mapped genes
12h-CK-1	38.07	36,976,258	32,381,211	87.57%	82.01%	35281
12h-CK-2	38.07	36,547,552	31,737,232	86.84%	81.82%	34782
12h-CK-3	38.07	36,309,778	31,468,060	86.67%	80.67%	35320
12h-KS-1	38.07	36,507,590	32,071,565	87.85%	83.38%	35352
12h-KS-2	38.07	36,763,226	32,059,054	87.20%	81.62%	35351
12h-KS-3	38.07	36,513,816	31,749,080	86.95%	81.41%	35429
96h-CK-1	38.07	36,886,386	32,109,249	87.05%	81.79%	35608
96h-CK-2	38.07	36,515,094	31,576,196	86.47%	81.72%	35270
96h-CK-3	38.07	36,494,576	31,449,058	86.17%	81.15%	35260
96h-KS-1	38.07	36,956,330	32,146,308	86.98%	81.33%	35807
96h-KS-2	38.07	36,737,316	32,133,744	87.47%	82.20%	36263
96h-KS-3	38.07	36,409,348	31,493,300	86.50%	81.31%	35141

Additional file 1: Table S1. RNA-Seq and qPCR results of 8 genes.

Gene ID	log ₂ (ks/ck)		Primer (forward/reverse)
	RNA-Seq	qPCR	
12h			
10024152	-2.697734106	-3.179931507	GACCAAGGACAATGCTACTCAAACCT CAAACCTAACCGTGTATCCCTCA
10021422	-2.812575003	-2.070599111	TGGGGATAGGAACATTGTAGGCA TGATTGGCACATCGTCCACATAA
10028689	2.647740432	1.276556142	GCATTAGCCACTGTTCCCTCCTTC ACCCTGTCGGTTCATCAAGTCA
10040830	2.454584375	1.898208872	AGGAAGAGGAGAAGAACGACAAGT GGGAACCGTAACAGTCAGCAC
96h			
10024511	1.30512419	0.447661972	CCTCAGGACGATCCAAGCAGTA CTTCTCGGTCACCATAGCCAAC
10013304	1.689218052	1.950688553	CGGCATCAAACCAACGAAG CAGAGTAAAGAGTAGAGTGCGAAGG
10024074	-2.047444922	-1.541110101	CCGAAATGGGGACACCTGA AACGCTGAACACGCTCCTGAC
10009092	-1.692589109	-0.923664092	GCTACAGGGGGAGCCTAATTTTC GGTGGTGTGCCGAGATAGATG

Table 2. Top 10 DEGs of different test sample.

Sample name	Gene ID	log ₂ FC (ks/ck)	Annotation
12h-up	MSTRG.23818.4	11.224	MATE efflux family protein 8-like,antiporter activity
	MSTRG.22451.40	10.8207	hypothetical protein JCGZ_23550,Aspartokinase
	MSTRG.25220.17	10.3759	ABC transporter family protein, P-loop containing nucleoside triphosphate hydrolase
	MSTRG.28462.4	9.9905	rop guanine nucleotide exchange factor 14
	MSTRG.651.2	9.9484	protein SMG7 isoform X1,mRNA surveillance pathway
	MSTRG.7917.2	9.854	hypothetical protein POPTR,IQ motif, EF-hand binding site
	MSTRG.21322.6	9.8472	2-alkenal reductase (NADP ⁽⁺⁾ -dependent)-like, Alcohol dehydrogenase
	MSTRG.7820.5	9.6922	DEAD-box ATP-dependent RNA helicase 31-like, Helicase
	MSTRG.9921.1	9.5619	hypothetical protein JCGZ_21293,Kinesin family member
	MSTRG.32525.1	9.5258	paired amphipathic helix protein Sin3-like 4 isoform X2,SIN3 transcription regulator homolog
12h-down	MSTRG.14003.5	-12.2798	hypothetical protein JCGZ_08504,Glycosyl hydrolase family
	MSTRG.25624.2	-11.5822	hypothetical protein POPTR,bZIP transcription factor
	MSTRG.26913.4	-10.9765	ATPase PDR2 isoform X2,P-type ATPase
	MSTRG.19680.3	-10.9212	hypothetical protein PRUPE,P-type ATPase
	MSTRG.29862.4	-10.7133	pre-mRNA-splicing factor RSE1 ,Cleavage and polyadenylation specificity factor
	MSTRG.22176.2	-10.6614	uncharacterized protein LOC105641844 isoform X1
	MSTRG.37077.2	-10.6254	transferase, transferring glycosyl groups, putative
	MSTRG.20859.3	-10.6097	branchpoint-bridging protein-like,RNA binding
	MSTRG.5716.3	-10.5711	BEACH domain-containing protein lvsA, catalytic activity
	MSTRG.17515.6	-10.3884	arginine/serine-rich splicing factor, putative
96h-up	MSTRG.5716.3	11.7055	BEACH domain-containing protein lvsA,catalytic activity
	MSTRG.25220.17	11.3277	ABC transporter family protein,P-loop containing nucleoside triphosphate hydrolase
	MSTRG.16740.3	10.6337	Ubiquinone biosynthesis protein coq-8, putative, Lipase LipE
	MSTRG.21781.1	10.2391	zinc finger CCCH domain-containing protein 5 isoform X2,aminotransferase
	MSTRG.24890.2	10.2207	paired amphipathic helix protein Sin3-like 2 isoform X1,SIN3 transcription regulator homolog
	MSTRG.13309.2	9.893	extracellular calcium sensing receptor, Rhodanese-like domain
	MSTRG.6782.4	9.615	ARF GTPase-activating domain-containing family protein, Endocytosis
MSTRG.9580.2	9.4647	hypothetical protein JCGZ_14917,Replication, recombination and repair	
96h-down	MSTRG.13838.1	9.4321	probable LRR receptor-like serine/threonine-protein kinase At1g06840 isoform X2, protein kinase APK1A
	MSTRG.31298.4	9.4203	conserved hypothetical protein, Histidine kinase-like ATPase
	MSTRG.15437.5	-10.8517	uncharacterized protein At4g37920
	MSTRG.22308.3	-10.0692	serine threonine-protein kinase
	MSTRG.33711.3	-9.9849	P-loop containing nucleoside triphosphate hydrolase
	MSTRG.36828.2	-9.9692	hypothetical protein POPTR_0010s21550g
	MSTRG.26561.1	-9.8794	protein TRANSPARENT TESTA 12-like,Mate efflux family protein
	MSTRG.29479.6	-9.7762	zinc finger family protein, cation binding
	MSTRG.14839.2	-9.7025	hypothetical protein JCGZ_01093
	MSTRG.4433.3	-9.5495	conserved hypothetical protein, PHOSphatase
	MSTRG.30486.10	-9.5261	uncharacterized protein LOC105126489 isoform X2
	MSTRG.10321.4	-9.5175	probable methyltransferase PMT9,methyltransferase

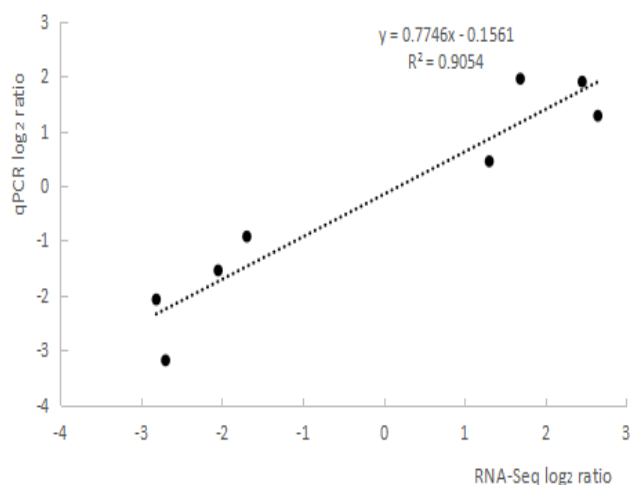


Fig. 1. Correlations between RNA-Seq and qPCR.

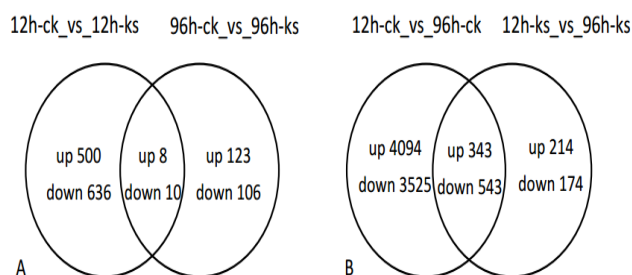


Fig. 2. Venn diagram of DEGs under K⁺ starvation in flax. A. Number of DEGs after treatment for 12 and 96h, B. Number of DEGs in control (ck) and K⁺ starvation (ks) treatment group.

Table 3. Top 15 signaling transduction protein families.

Gene family	Num.	Annotation
APRR	20	Signal transduction response regulator
CIPK	19	CBL-interacting protein kinase
P2C	10	protein phosphatase 2
TMVRN	10	TMV resistance protein N-like
ARR	8	Transmembrane amino acid transporter protein
AI5L	7	Abscisic acid responsive elements-binding factor 2
LAX	7	auxin transporter-like protein
PI5K	7	phosphatidylinositol-4-phosphate 5-kinase
TGA	7	Basic-leucine zipper domain
CCD	6	Cyclin, N-terminal domain
AHK	5	cytokinin receptor 1B,Histidine kinase-like ATPase
EBF	5	EIN3-binding F-box protein
GH3	5	probable indole-3-acetic acid-amido synthetase
RAC	5	Small GTPase superfamily

Table 4. Numbers of channel DEGs in each comparison group.

Channels	Num. of each group			
	12h-ck vs 96h-ck	12h-ks vs 96h-ks	12h-ck vs 12h-ks	96h-ck vs 96h-ks
AKT	1	0	0	0
KAT	3	1	1	0
CNG	6	5	4	0

A Venn diagram was constructed to identify the same and different DEGs between the two potassium starvation time points (Fig. 2A). A total of 18 genes responded with

changes in expression in both periods. Of these, 8 genes (Additional file 2: Table S2) were up to the expression and 10 genes (Additional file 3: Table S3) were down to the expression, showing 18 genes might take significant effects in the entire K⁺ starvation period.

The other Venn diagram shows the DEGs between different potassium starvation periods (Fig. 2B). Comparison of these results eliminates the natural variability of genes expression associated with time and growth. In both ck and ks groups, 886 genes responded of 343 genes were up to the expression, and 543 genes were down to the expression.

Additional file 2: Table S2. The common up-regulated differentially expressed genes of 12h-ck_vs_12h-ks and 96h-ck_vs_96h-ks.

Gene	log2. Fold change	Gene	log2. Fold change
MSTRG.34278.1	1.12	MSTRG.19459.1	1.58
MSTRG.34223.1	2.78	MSTRG.8623.1	3.31
MSTRG.25220.17	10.38	MSTRG.14519.1	1.40
MSTRG.17749.2	9.26	MSTRG.9727.3	2.35

Additional file 3: Table S3. The common down-regulated differentially expressed genes of 12h-ck_vs_12h-ks and 96h-ck_vs_96h-ks.

Gene	log2. Fold change	Gene	log2. Fold change
MSTRG.18807.2	-5.54	MSTRG.32260.1	-2.59
MSTRG.19646.4	-1.42	MSTRG.7135.1	-8.03
MSTRG.33711.3	-8.31	MSTRG.20087.1	-1.10
MSTRG.2149.1	-1.64	MSTRG.16196.1	-1.06
MSTRG.28900.3	-1.22	MSTRG.22964.1	-5.78

Functional note of DEGs in clusters: To reveal definite functions of DEGs, GO and KEGG pathway enrichment analysis of DEGs were carried out. GO functional enrichment analysis showed that for either 12h-ks vs 12h-ck or 96h-ks vs 96h-ck comparisons, DEGs were mainly concentrated in five functional categories including metabolic process, cellular process, single-organism process, catalytic activity and binding function terms (Fig. 3).

After potassium starvation for 12h, KEGG enrichment indicated DEGs were chiefly concentrated in energy metabolism, carbohydrate metabolism, carbon metabolism, amino acid metabolism and terpenoids metabolism and polyketides metabolism (Fig. 4). After potassium starvation for 96h, significantly enriched KEGG pathways included lipid metabolism, carbohydrate metabolism, amino acid metabolism, terpenoids metabolism, polyketides metabolism, metabolism of cofactors and vitamins and energy metabolism. In addition, both incubation durations exhibited DEGs enriched into signal transduction pathway.

Analysing the DEGs: During the process of long-term evolution, plants have formed sets of complex and effective mechanisms to adapt to and resist various biological and abiotic stresses. Transcriptional regulation of gene expression usually plays all kinds of important roles in plant stress response processes. After transcription factor annotation of DEGs was conducted for the two stress duration periods tested, 546 DEGs were

annotated to 46 TFs families (Fig. 5), most of which belonged to MYB-related, bHLH, NAC, B3, bZIP, WRKY, ERF and other transcription factor families.

For DEGs exhibiting comparable expression across all four groups, 262 DEGs were annotated to signal transduction proteins or to proteins that participate in signal transduction pathways, including APRR, CIPK, P2C and other signaling channels (Table 3, Additional file 4: Table S4).

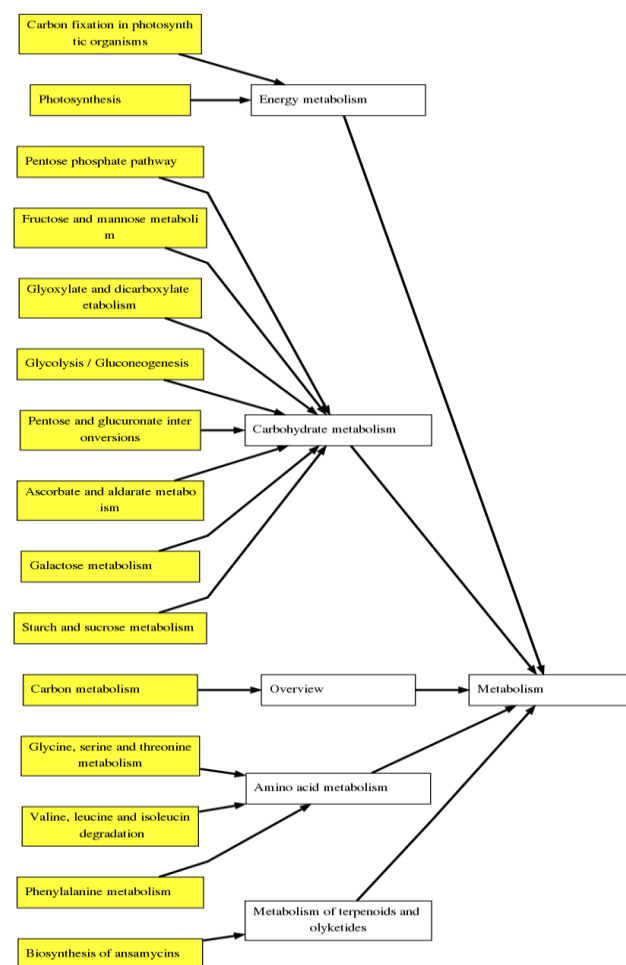


Fig. 4. KEGG pathway enrichment analysis of the DEGs after 12h K⁺ starvation.

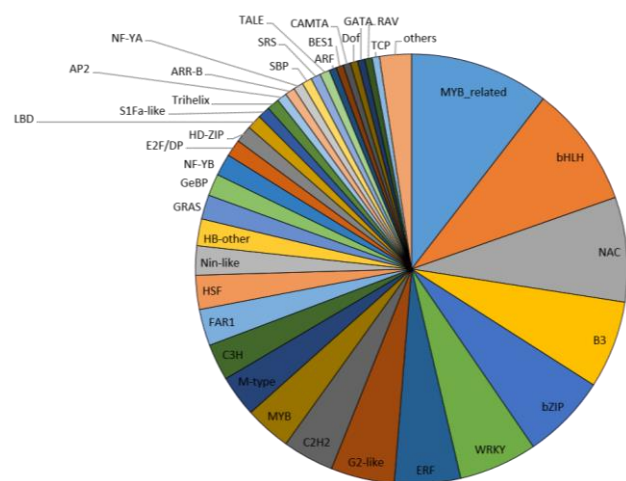


Fig. 5. Transcription factors annotation of the DEGs.

For DEGs exhibiting contrasting expression levels among the groups, 102 DEGs were annotated to the hormone response protein function, including 17 ABA response proteins such as NCED/ZEP, 16 ethylene response proteins such as MAC OS/ACS, 22 auxin response proteins such as AUX, 10 JA response proteins such as LOX/OPR and 38 cytokinin response proteins such as AHP/ARR/Homeobox protein/IPT, among others (Additional file 5-9: Tables S5-9).

In addition, 106 genes were annotated to transporter function, including 13 Ca/P/N/S transporter CAXs, 5 NRTs and 88 ABC transporters (Additional file 10-12: Tables S10-12).

Multiple ion channels were also identified in the DEGs, including AKT channels (MSTRG.35780.2), KAT channels and CNG ion channels (Table 4, Additional file 13-14: Tables S13-14). In addition, the SNARE protein (Additional file 15: Table S15) was also detected.

In the comparison of 12h groups, some HSPs were found that exhibited gene expression trends that were mainly up-regulated (14), with only 2 HSPs down-regulated; in the comparison of 96h groups, only one down-regulated HSP protein was identified (Additional file 16: Table S16).

Discussion

For DEGs exhibiting markedly different expression levels among the four groups, a large number of transcription factors were identified, suggesting that TFs are the most important group of regulatory factors in plants. This result aligns with other recent reports describing numerous plant TFs that have been experimentally confirmed to associate with biological and abiotic stress responses. For example, MYB transcription factors participate in regulating numerous physiological processes, for example plant growth and development, physiological metabolism, cell morphology and cell differentiation. At the same time, the MYB protein family is also involved in responses to abiotic stress (Rubio *et al.*, 2001). Notably, the MYB-type transcription factor regulates rice high-affinity potassium transporter1; 1 (Wang *et al.*, 2015), while low K⁺ stress induces expression of all three OsHKT genes in roots (Horie *et al.*, 2010). In this study, 76 MYB-related DEGs were also identified as candidate DEGs for future flax potassium stress studies. Other plant transcription factors, bHLH, WRKY and NAC, also play very important roles in plant development, stress responses, defense responses and secondary metabolism. Overall, 50 bHLH, 32 WRKY and 43 NAC transcription factors were identified in this study. Expression of bHLH participates in development of both epidermal and root hairs and regulates signal transduction and morphological changes in response to light. The WRKY transcription factor family participates in many physiological plant processes and makes a significant effect in stress resistance (Long *et al.*, 2010). NAC gene widely participates in growth, biological and non-biological stress responses. In addition, DEGs of 27

ERF transcription factors belonging to the ERF family were also identified in this study. ERF, AP2Z and RAV families all belong to the AP2/ERF transcription factor super family. In the future, gene cloning, transgenic studies and gene function verification should be further conducted for the understanding of these plant regulatory networks.

In our analysis of flax DEGs at 12h and 96h for potassium stress, numerous genes were enriched. Many genes were involved in energy metabolism, carbohydrate metabolism and amino acid metabolic pathways. For example, the pentose phosphate pathway is closely related to plant growth and responses to various environmental stresses. Energy-related proteins are involved in substance accumulation and energy metabolism in leaves during photosynthesis and adapt to a various physiological and biochemical pathways through light signal transmission processes (Von *et al.*, 2003). Plant hormones are also widely involved in physiological and biochemical responses to adverse stresses. Ethylene is one of several important signal molecules in plant responses to abiotic stress, which can activate downstream gene expression by binding to primary transcription factors such as the ethylene receptor to trigger ethylene responses (Li *et al.*, 2015). Auxins can induce rapid and instantaneous high expression of genes such as ARF/AUX/GH3 in plant stress responses (Wang *et al.*, 2010a). ABA acts as a central mediator of information transfer between plant underground-aboveground parts, inducing changes in cell turgor pressure by activating Ca^{2+} , K^+ , anion channels and adjusting the paths of ions into and out of cells (Milborrow *et al.*, 1997). Plant hormones also interact with each other, providing a basis for regulation of the hormone regulation network. Many studies have shown that ethylene and auxin play important roles in directing development of root morphology in response to

low potassium stress by inhibiting growth of the main root while stimulating root hair elongation. In fact, root morphology of plants grown with low potassium resembles growth in response to exogenous ethylene and auxin treatment (Muday *et al.*, 2012). Moreover, related gene expression of ethylene synthesis genes and signal transduction have been reported under low potassium conditions (Shin *et al.*, 2005). In this study, 16 ethylene DGEs, 22 auxin DGEs and 17 ABA DGEs were discovered. This research established a foundation that revealed molecular mechanisms linking plant hormone responses to low potassium stress responses.

K^+ channels also play a role in stress responses and are classified into three categories according to their diverse structures and functions: the shaker family, KCO family and other channels. The shaker family channel was one of the earliest discovered pathways in plant cells, including the AKT/HAK ion channel (Kim *et al.*, 2010), identified in this study also (MSTRG.35780.2). Another plant channel, the CNG channel, incorporates 6 transmembrane zones that structurally resemble the transmembrane zones of the shaker family represented by 15 DEGs (Additional file 14: Table S14) identified in this study. In addition, 10 DEGs matching SNARE proteins (Additional file 15: Table S15), which promote the formation of plant cell plates and interact with ion channel proteins (Bao *et al.*, 2005), were identified. DEGs were also identified that code for thermophyton and related proteins, which repair plant stress damage and degrade damaged proteins. Interestingly, because of their short-term expressive characteristics (Krebs *et al.*, 2001), in this study, the number of the thermal shock proteins in 96h group (only 1 down-regulate HSP proteins) was less than that of the 12h group (14 up-regulated HSP proteins and 2 HSPs down-regulate) (Additional file 16: Table S16).

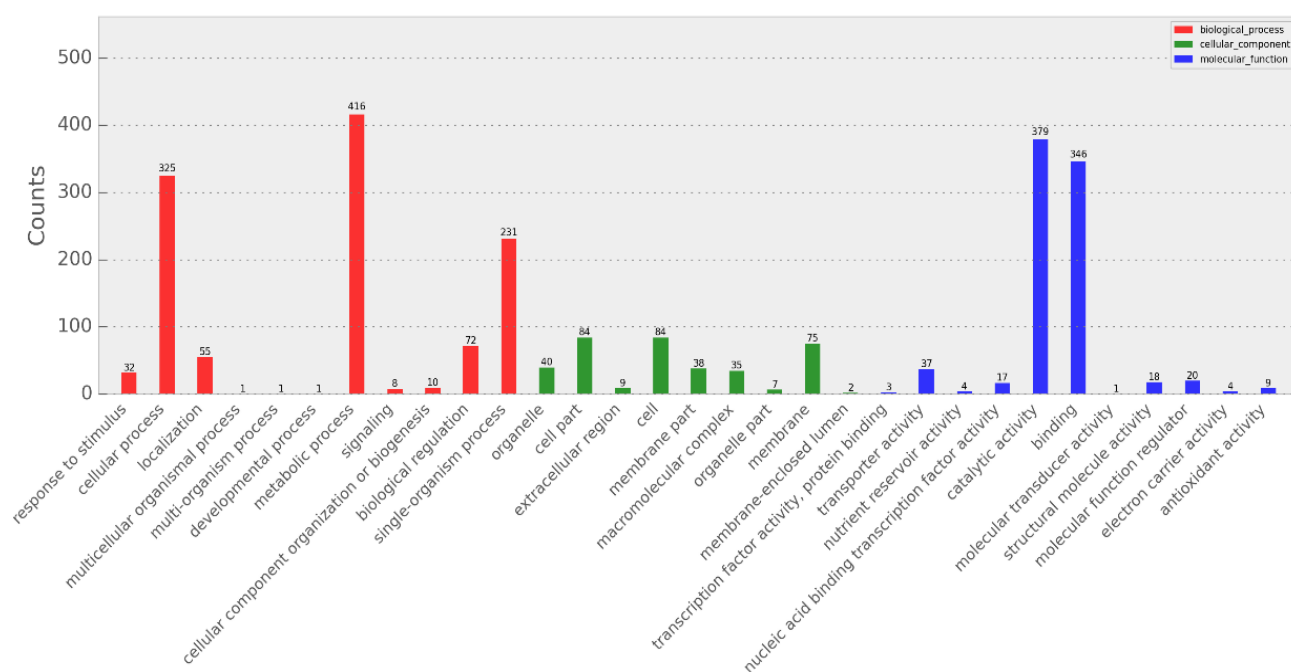


Fig. 3. GO enrichment analysis of the DEGs after 12h K^+ starvation.

Additional file 4: Table S4. 262 DEGs were noted to signal transduction proteins or participate in signal transduction pathways.

Gene	Gene family	Num.	Annotation
APRR1 APRR2 APRR5 APRR7	APRR	20	Signal transduction response regulator
CIPK1 CIPK2 CIPK3 CIPK6 CIPK8 CIPK9 CIPKA CIPKB CIPKH CIPKP	CIPK	19	CBL-interacting protein kinase
P2C03 P2C06 P2C08 P2C24 P2C51 P2C56	P2C	10	protein phosphatase 2
TMVRN	TMVRN	10	TMV resistance protein N-like
ARR1 ARR3 ARR4 ARR8 ARR9	ARR	8	Transmembrane amino acid transporter protein
AI5L4 AI5L5 AI5L7	AI5L	7	Abscisic acid responsive elements-binding factor 2
LAX2 LAX5	LAX	7	auxin transporter-like protein
PI5K7 PI5K8 PI5K9	PI5K	7	phosphatidylinositol-4-phosphate 5-kinase
TGA1 TGA21 TGA4	TGA	7	Basic-leucine zipper domain
CCD31 CCD32	CCD	6	Cyclin, N-terminal domain
AHK2 AHK3 AHK4	AHK	5	cytokinin receptor 1B,Histidine kinase-like ATPase
EBF1 EBF2	EBF	5	EIN3-binding F-box protein
GH31 GH35	GH3	5	probable indole-3-acetic acid-amido synthetase
RAC1 RAC2 RAC7	RAC	5	Small GTPase superfamily
SRK2B SRK2E	SRK2	5	serine/threonine-protein kinase
XLG1 XLG2 XLG3	XLG	5	guanine nucleotide binding protein (G protein)
BRI1	BRI1	4	Leucine-rich receptor-like protein kinase family protein
CTR1	CTR1	4	serine/threonine-protein kinase CTR
GID1C	GID1C	4	alpha beta hydrolase fold-3 domain protein
IAA13 IAA14 IAA16 IAA26	IAA	4	auxin-induced protein
SAPK2 SAPK3	SAPK	4	serine threonine-protein kinase
SPG1	SPG1	4	Septum-promoting GTP-binding, Potassium voltage-gated channel
2A5B 2A5G 2A5I	2A5	3	serine/threonine protein phosphatase
AX15A AX22D	AX15A/AX22D	3	auxin-induced protein
BKI1	BKI1	3	BRI1 kinase inhibitor 1-like
ERD2 ERD22	ERD	3	ER lumen protein retaining receptor
ERF92	ERF92	3	Ethylene-responsive transcription factor 1B
FAB1B FAB1C	FAB1	3	putative 1-phosphatidylinositol-3-phosphate 5-kinase
NPR3	NPR3	3	Regulatory protein NPR1, putative
RGAP1 RGAP2	RGAP	3	GTPase Activating protein
SR54C	SR54C	3	signal recognition particle protein, putative
TIF6B	TIF6B	3	Posttranslational modification
TATA TATB	TAT	3	Sec-independent protein translocase protein TatA, Part of the twin-arginine translocation (Tat) system
AUX28	AUX28	2	IAA family
CDS4	CDS4	2	phosphatidate Cytidylyltransferase
CFTSY	CFTSY	2	Signal recognition particle, SRP54 subunit, helical bundle
DGK1 DGK5	DGK	2	Diacylglycerol Kinase
EIL3	EIL3	2	ETHYLENE-INSENSITIVE3-like 3 family protein
GLR36 GLRX	GLR36/GLRX	2	glutamate receptor
IPPK	IPPK	2	inositol 1,3,4,5,6-pentakisphosphate 2-kinase
LTD	LTD	2	Ankyrin repeat-containing domain
MIRO1 MIRO2	MIRO	2	rac-GTP binding protein, putative
MYC2 MYC4	MYC	2	Myc-type, basic helix-loop-helix (bHLH) domain
PIF5	PIF5	2	PREDICTED: transcription factor PIF4

Additional file 4: Table S4. (Cont'd).

Gene	Gene family	Num.	Annotation
PLSP1	PLSP1	2	Signal peptidase i
RAF2A RAF2B	RAF2	2	PREDICTED: ras-related protein
SIPL2	SIPL2	2	Signal peptide peptidase-like 2 isoform 1
SRPR	SRPR	2	PREDICTED: signal recognition particle receptor subunit alpha-like isoform X1
TIR	TIR	2	interleukin-1 receptor homology (TIR) domain
CDI	CDI	2	Part of the twin-arginine translocation (Tat) system
AFB3	AFB3	1	hypothetical protein POPTR_0004s03400g
AFP2	AFP2	1	RNA binding protein, putative
AHP1	AHP1	1	PREDICTED: histidine-containing phosphotransfer protein 1-like
AMRA1	AMRA1	1	PREDICTED: uncharacterized protein LOC105125661 isoform X1
AP2A2	AP2A2	1	hypothetical protein JCGZ_11239
ARFRP	ARFRP	1	ADP-ribosylation factor, putative
ARG7	ARG7	1	PREDICTED: indole-3-acetic acid-induced protein ARG7-like
ASCC2	ASCC2	1	hypothetical protein JCGZ_16037
BIG5	BIG5	1	PREDICTED: brefeldin A-inhibited guanine nucleotide-exchange protein 5
BZR1	BZR1	1	BRASSINAZOLE-RESISTANT 1 protein, putative
CABO	CABO	1	Ca ²⁺ -binding protein 1
CALM7	CALM7	1	PREDICTED: calmodulin-7 isoform X1
CML10	CML10	1	Ca ²⁺ -binding protein 1
CNIH4	CNIH4	1	PREDICTED: protein cornichon homolog 4
COI1	COI1	1	RNI-like superfamily protein
DPNP1	DPNP1	1	hypothetical protein POPTR_0007s04240g
EIN2	EIN2	1	hypothetical protein JCGZ_16519
GAI	GAI	1	PREDICTED: DELLA protein GAI-like
GBF4	GBF4	1	PREDICTED: G-box-binding factor 4
HBP1C	HBP1C	1	Transcription factor HBP-1b(c1), putative
HIS7	HIS7	1	hypothetical protein POPTR_0009s12340g
IMPL1	IMPL1	1	myo inositol monophosphatase, putative
ITPK3	ITPK3	1	hypothetical protein PHAVU_007G047700g
LST8	LST8	2	PREDICTED: protein LST8 homolog isoform X1
NLE1	NLE1	1	PREDICTED: notchless protein homolog
ORR26	ORR26	1	PREDICTED: two-component response regulator ARR11-like
PLCD2	PLCD2	1	hypothetical protein JCGZ_01271
PRR1	PRR1	1	PREDICTED: two-component response regulator-like APRR1
PWP2	PWP2	1	signal transduction protein with Nacht domain
RAE1C	RAE1C	1	Potassium voltage-gated channel
RAN3	RAN3	1	Small GTP-binding protein domain
SAU24	SAU24	1	PREDICTED: indole-3-acetic acid-induced protein ARG7-like
SNC1	SNC1	1	PREDICTED: toll/interleukin-1 receptor-like protein
SPCS2	SPCS2	1	PREDICTED: probable signal peptidase complex subunit 2
TAO1	TAO1	1	hypothetical protein POPTR_0019s09620g
THOC3	THOC3	1	PREDICTED: THO complex subunit 3
VTC4	VTC4	1	myo inositol monophosphatase, putative
Y4117	Y4117	1	PREDICTED: TMV resistance protein N-like
Y4523	Y4523	1	kinase family protein

Additional file 5: Table S5. 17 ABA response proteins.

Gene	Gene	Gene	Gene
MSTRG.12261.1	MSTRG.25673.1	MSTRG.30808.1	MSTRG.40442.1
MSTRG.10668.1	MSTRG.28891.1	MSTRG.31862.1	MSTRG.4828.1
MSTRG.1437.1	MSTRG.28922.1	MSTRG.31862.2	MSTRG.4971.1
MSTRG.14956.1	MSTRG.28922.2	MSTRG.34700.1	MSTRG.4988.1
MSTRG.24726.1			

Additional file 6: Table S6. 16 ethylene response proteins.

GENE	log2. Fold change	GENE	log2. Fold change
MSTRG.21647.1	-2.08	MSTRG.26417.3	-6.86
MSTRG.4489.2	-3.25	MSTRG.29690.1	-1.50
MSTRG.4489.1	-2.43	MSTRG.31262.2	-1.11
MSTRG.7666.1	1.19	MSTRG.23921.4	-4.14
MSTRG.25779.2	-1.97	MSTRG.21647.1	-1.19
MSTRG.25779.1	-1.03	MSTRG.26200.6	1.40
MSTRG.26417.1	-1.12	MSTRG.4766.3	-8.08
MSTRG.13127.1	8.02	MSTRG.13053.5	-7.60

Additional file 7: Table S7. 22 auxin response proteins.

Gene	Gene	Gene	Gene
MSTRG.12741.1	MSTRG.24513.1	MSTRG.35527.1	MSTRG.5734.2
MSTRG.17016.1	MSTRG.2522.1	MSTRG.36168.1	MSTRG.6424.1
MSTRG.19759.1	MSTRG.26656.1	MSTRG.36872.2	MSTRG.6424.2
MSTRG.2100.1	MSTRG.29326.1	MSTRG.4702.1	MSTRG.7513.2
MSTRG.2113.1	MSTRG.30172.4	MSTRG.539.1	MSTRG.7683.3
MSTRG.22511.1	MSTRG.33390.2		

Additional file 8: Table S8. 10 JA response proteins.

Gene	Gene	Gene	Gene
MSTRG.1151.3	MSTRG.24428.1	MSTRG.34761.1	MSTRG.9645.1
MSTRG.1151.4	MSTRG.25480.1	MSTRG.36748.1	MSTRG.9646.2
MSTRG.20941.1	MSTRG.32402.1		

Additional file 9: Table S9. 38 cytokinins response proteins.

Gene	Gene	Gene	Gene
MSTRG.10338.1	MSTRG.21656.1	MSTRG.29826.1	MSTRG.7236.1
MSTRG.10900.1	MSTRG.22334.1	MSTRG.31765.1	MSTRG.7236.3
MSTRG.1221.1	MSTRG.22417.4	MSTRG.32458.1	MSTRG.7236.4
MSTRG.12554.1	MSTRG.24168.1	MSTRG.33741.1	MSTRG.7365.1
MSTRG.13261.1	MSTRG.25536.1	MSTRG.35378.4	MSTRG.7656.1
MSTRG.16899.1	MSTRG.25736.1	MSTRG.36570.1	MSTRG.8341.1
MSTRG.17892.2	MSTRG.2837.1	MSTRG.36772.1	MSTRG.8928.1
MSTRG.1965.1	MSTRG.28984.1	MSTRG.4481.1	MSTRG.9154.1
MSTRG.20809.1	MSTRG.29066.1	MSTRG.5703.1	MSTRG.9618.1
MSTRG.20809.2	MSTRG.29418.1		

Additional file 10: Table S10. 13 Ca/P/N/S transporter CAXs were annotated to the transporter.

Gene	Gene	Gene	Gene
MSTRG.22970.2	MSTRG.13144.1	MSTRG.16821.20	MSTRG.22970.4
MSTRG.10423.1	MSTRG.18898.3	MSTRG.16821.18	MSTRG.13144.2
MSTRG.22970.3	MSTRG.18898.5	MSTRG.22970.3	MSTRG.36436.1
MSTRG.10423.1			

Additional file 11: Table S11. 5 NRTs were annotated to the transporter.

Gene	Gene	Gene	Gene
MSTRG.32010.1	MSTRG.10725.2	MSTRG.8652.1	MSTRG.29985.1
MSTRG.15321.1			

Additional file 12: Table S12. 88 ABC transporters were annotated to the transporter.

Gene	Gene	Gene	Gene
MSTRG.21562.2	MSTRG.18886.2	MSTRG.25220.25	MSTRG.35122.1
MSTRG.10088.1	MSTRG.18887.1	MSTRG.25424.1	MSTRG.35250.1
MSTRG.10203.2	MSTRG.19476.4	MSTRG.26891.12	MSTRG.35554.1
MSTRG.10203.3	MSTRG.19902.1	MSTRG.27027.1	MSTRG.35788.1
MSTRG.10844.1	MSTRG.20938.1	MSTRG.27205.1	MSTRG.36321.1
MSTRG.10844.2	MSTRG.21562.1	MSTRG.27205.3	MSTRG.36820.1
MSTRG.10988.9	MSTRG.21562.2	MSTRG.27671.1	MSTRG.3703.1
MSTRG.11065.1	MSTRG.21627.2	MSTRG.28250.1	MSTRG.37184.1
MSTRG.11514.4	MSTRG.22149.1	MSTRG.29062.11	MSTRG.40398.1
MSTRG.11520.1	MSTRG.22149.2	MSTRG.29159.4	MSTRG.5655.1
MSTRG.12553.1	MSTRG.22149.3	MSTRG.29399.1	MSTRG.5655.2
MSTRG.12876.2	MSTRG.22149.4	MSTRG.29399.2	MSTRG.6654.1
MSTRG.12876.3	MSTRG.22944.3	MSTRG.29399.3	MSTRG.6726.1
MSTRG.12877.1	MSTRG.22944.6	MSTRG.29524.1	MSTRG.6727.1
MSTRG.14615.1	MSTRG.22944.9	MSTRG.29810.1	MSTRG.8003.1
MSTRG.14819.6	MSTRG.24650.1	MSTRG.31309.1	MSTRG.8183.1
MSTRG.16296.1	MSTRG.24772.1	MSTRG.32006.3	MSTRG.8183.4
MSTRG.16839.1	MSTRG.24772.2	MSTRG.32603.1	MSTRG.8183.5
MSTRG.16881.1	MSTRG.24773.1	MSTRG.3406.1	MSTRG.8185.1
MSTRG.17555.1	MSTRG.24774.1	MSTRG.34304.1	MSTRG.8512.4
MSTRG.18318.1	MSTRG.24774.2	MSTRG.34405.3	MSTRG.9375.1
MSTRG.18501.2	MSTRG.25220.17	MSTRG.34494.1	MSTRG.9987.1

Additional file 13: Table S13. 5 KAT channels.

Gene	Gene	Gene	Gene
MSTRG.21106.2	MSTRG.35604.1	MSTRG.21106.2	MSTRG.19910.1
MSTRG.19910.1			

Additional file 14: Table S14. 15 CNG ion channels.

Gene	Gene	Gene	Gene
MSTRG.16570.5	MSTRG.16570.5	MSTRG.26083.4	MSTRG.20976.1
MSTRG.26083.1	MSTRG.19154.1	MSTRG.28377.4	MSTRG.26083.1
MSTRG.36504.1	MSTRG.19157.2	MSTRG.16570.5	MSTRG.8011.2
MSTRG.36504.3	MSTRG.20976.1	MSTRG.16570.6	

Additional file 15: Table S15. 10 SNARE protein.

Gene	Gene	Gene	Gene
MSTRG.31947.1	MSTRG.3952.1	MSTRG.25185.1	MSTRG.22229.1
MSTRG.31947.1	MSTRG.1429.1	MSTRG.19724.1	MSTRG.31947.1
MSTRG.16238.1	MSTRG.32713.1		

Additional file 16: Table S16. 17 HSP proteins.

ck_vs_ks	Gene	log2. Fold change
12h-ck_vs_12h-ks	MSTRG.11475.1	2.47
12h-ck_vs_12h-ks	MSTRG.21721.1	1.89
12h-ck_vs_12h-ks	MSTRG.6623.1	2.38
12h-ck_vs_12h-ks	MSTRG.25677.1	2.47
12h-ck_vs_12h-ks	MSTRG.5016.1	1.80
12h-ck_vs_12h-ks	MSTRG.27147.1	4.44
12h-ck_vs_12h-ks	MSTRG.6956.1	1.76
12h-ck_vs_12h-ks	MSTRG.18054.1	1.63
12h-ck_vs_12h-ks	MSTRG.33742.1	3.18
12h-ck_vs_12h-ks	MSTRG.35588.1	1.85
12h-ck_vs_12h-ks	MSTRG.22290.1	4.67
12h-ck_vs_12h-ks	MSTRG.5016.3	1.13
12h-ck_vs_12h-ks	MSTRG.19205.1	1.31
12h-ck_vs_12h-ks	MSTRG.5016.2	1.73
12h-ck_vs_12h-ks	MSTRG.31232.1	-1.16
12h-ck_vs_12h-ks	MSTRG.11719.2	-8.40
96h-ck_vs_96h-ks	MSTRG.20014.5	-1.05

Conclusions

In order to study the effect of low potassium stress on flax, a series of RNA expression profiles was analyzed from plants subjected to potassium starvation for 12h and 96h. Twelve samples were sequenced by Illumina HiSeq platform, generating about 4.58Gb sequence each sample. After mapping sequenced reads to the reference genome and reconstructed transcripts, 33287 novel transcripts were obtained. 24219 were sequences demonstrating previously unknown splicing events for known genes, 3687 were novel coding transcripts without any known features and 5381 were derived from long non coding RNAs. The qRT-PCR results showed sequencing data meet the accuracy requirement. During potassium starvation for 12h and 96h, 18 genes were co-expressed; GO function enrichment analysis showed DEGs were mainly concentrated in five functional categories; KEGG pathway enrichment analysis revealed different pathways. Predominant expression of transcription factors was observed in flax potassium starvation response, while numerous DEGs coding for signal transduction proteins or for participating proteins in signal transduction pathways, hormone responses and transporters were discovered. Multiple ion channel DEGs were identified, including AKT channels, KAT channels and CNG ion channels. In addition, DEGs for several HSPs were detected as part of the short-term stress response to potassium starvation. As the first study to analyze the flax transcriptome under K⁺ deficiency, this report reveals numerous candidate genes for examination in future studies. Such studies should help to elucidate molecular mechanisms involved in adaptation of flax and other plants to potassium deficiency.

Acknowledgements

This work was supported by the earmarked fund for National Key R&D Program of China (No. 2018YFD0201100), the 13th Five-Year Key Research and Development Program of China (Grant No. 2017YFD0201000), Modern Agro-industry Technology Research System (Grant No. CARS-16-E04), Reserved Leader Fund of Heilongjiang Province Leading Talent Echelon and Harbin's Youth Reserve Talents Project (Grant No. 2016RQQYJ113). This study was carried out on the Northeast Flax Scientific Observation Experimental Station of Ministry of Agriculture and Flax Branch of the National Bast Fiber Germplasm Improvement Center.

References

- Anders, S., D.J. McCarthy, Y. Chen, M. Okoniewski, G.K. Smyth, W. Huber and M.D. Robinson. 2013. Count-based differential expression analysis of RNA sequencing data using R and Bioconductor. *Nat. Protocols*, 8(9): 1765-1786.
- Bañuelos, M.A., B. Garcíadeblas, B. Cubero and N.A. Rodríguez. 2002. Inventory and functional characterization of the HAK potassium transporters of rice. *Plant Physiol.*, 130(2): 784-795.
- Bao, Y., Z. Wang and H. Zhang. 2005. Structure and function of SNAREs in plant. *Chinese Bull. Bot.*, 22.
- Cock, P.J., C.J. Fields, N.Goto, M.L. Heuer and P.M. Rice. 2010. The Sanger FASTQ file format for sequences with quality scores, and the Solexa/Illumina FASTQ variants. *Nucl. Acids Res.*, 38(6): 1767-1771.
- Epstein, E., D.W. Rains and O.E. Elzam. 1963. Resolution of dual of mechanisms of potassium absorption by barley roots. *Proceedings of the National Academy of Sciences of the United States of America*, 49(5): 684-692.

- Fan, M., Y. Huang, Y.Q. Zhong, Q.S. Kong, J.J. Xie, M.L. Niu, Y. Xu and Z.L. Bie. 2014. Comparative transcriptome profiling of potassium starvation responsiveness in two contrasting watermelon genotypes. *Planta*, 239: 397-410.
- Gao, X., M.A. Wen, Y. Cui, R. Wang and F. Zheng. 2000. Changes of soil nutrient contents and input of nutrients in arable of China. *Plant Nutr. & Fertilizer Sci.*, 6(4): 363-369.
- Horie, T., K. Yoshida, H. Nakayama, K. Yamada and S. Oiki. 2010. Two types of HKT transporters with different properties of Na⁺ and K⁺ transport in *Oryza sativa*. *Plant J.*, 27(2): 129-138.
- Jin, J., H. Zhang, L. Kong, G. Gao and J. Luo. 2014. Plant TFDB 3.0: a portal for the functional and evolutionary study of plant transcription factors. *Nucl. Acids Res.*, 42: 1182-1187.
- Kim, D., G. Perteau, C. Trapnell, H. Pimentel, R. Kelley and S.L. Salzberg. 2013. TopHat2: accurate alignment of transcriptomes in the presence of insertions, deletions and gene fusions. *Genome Biol.*, 14(4): R36.
- Kim, M.J., S. Ciani and D.P. Schachtman. 2010. A Peroxidase contributes to ROS production during Arabidopsis root response to potassium Deficiency. *Mol. Plant*, 3(2): 420-427.
- Krebs, R.A. and S.H. Holbrook. 2001. Reduced enzyme activity following Hsp70 overexpression in *Drosophila melanogaster*. *Biochem. Genetics*, 39(1-2): 73.
- Lan, W.Z., S.C. Lee, Y.F. Che, Y.Q. Jiang and S. Luan. 2011. Mechanistic analysis of AKT1 regulation by the CBL-CIPK-PP2CA interactions. *Mol. Plant*, 4(3): 527-536.
- Langmead, B. and S.L. Salzberg. 2012. Fast gapped-read alignment with Bowtie 2. *Nature Methods*, 9(4): 357-359.
- Li, B. and C.N. Dewey. 2011. RSEM: accurate transcript quantification from RNA-Seq data with or without a reference genome. *BMC Bioinform.*, 12(1): 323.
- Li, C.F., M. Li and K.R. Wang. 1998. The mechanism of potassium influence on the yield and quality of fiber flax. *J. Northeast Agri. Uni.*, 29(1): 21-26 (Chinese with English abstract).
- Li, W., M. Ma, Y. Feng, H.J. Li, Y.C. Wang, Y.T. Ma, M.Z. Li, F.Y. An and H.W. Guo. 2015. EIN2-directed translational regulation of ethylene signaling in Arabidopsis. *Cell*, 163(3): 670-683.
- Liu, G.D. and G.L. Liu. 2002. Screening indica rice for K-efficient genotypes. *Acta Agron. Sin.*, 28: 161-166.
- Long, T.A., H. Tsukagoshi, W. Busch, B. Lahner, D.E. Salt and P.N. Benfeya. 2010. The bHLH transcription factor POPEYE regulates response to iron deficiency in Arabidopsis roots. *Plant Cell*, 22(7): 2219-2236.
- Lu, L.M., Y. Chen, L. Lu, Y. Lu and L. Li. 2015. Transcriptome analysis reveals dynamic changes in the gene expression of tobacco seedlings under low potassium stress. *J. Gen.*, 94(3): 397-406.
- Ma, T.L., W.H. Wu and Y. Wang. 2012. Transcriptome analysis of rice root responses to potassium deficiency. *BMC Plant Biol.*, 12: 161.
- Mao, J., M.S.M. Nuruzzaman, S. Shi, J.T. Chao, Y.R. Jin, Q. Wang and H.B. Liu. 2016. Mechanisms and physiological roles of the CBL-CIPK networking system in *Arabidopsis thaliana*. *Genes*, 7(9): 62.
- Milborrow, B.V., R.S. Burden and H.F. Taylor. 1997. The conversion of 2-cis-[14C] Xanthoxic acid into [14C]ABA. *Phytochem.*, 45(2): 257-260.
- Muday, G.K., A. Rahman and B.M. Binder. 2012. Auxin and ethylene: collaborators or competitors? *Trens Plant Sci.*, 17(4): 181-195.
- Munns, R. and M. Tester. 2008. Mechanisms of salinity tolerance. *Ann. Rev. Plant Biol.*, 59(1): 651-681.
- Munson, R.D. 1985. Potassium in agriculture. Madison: ASA/CSSA/SSSA. pp. 754-794.
- Perteau, M., G.M. Perteau, C.M. Antonescu, T.C. Chang, J.T. Mendel and S.L. Salzberg. 2015. StringTie enables improved reconstruction of a transcriptome from RNA-seq reads. *Nature Biotechnol.*, 33(3): 290-295.
- Pettigrew, W.T. 2008. Potassium influences on yield and quality production for maize, wheat, soybean and cotton. *Physiologia Plantarum*, 133(4): 670-681.
- Ruan, L., J.B. Zhang, X.L. Xin, C.Z. Zhang, D.H. Ma, L. Chen and B.Z. Zhao. 2015. Comparative analysis of potassium deficiency-responsive transcriptomes in low potassium susceptible and tolerant wheat (*Triticum aestivum* L.). *Scientific Reports*, 5: 10090.
- Rubio, F., M.G.E. Santa and N.A. Rodríguez. 2010. Cloning of Arabidopsis, and barley cDNAs encoding HAK potassium transporters in root and shoot cells. *Physiologia Plantarum*, 109(1):34-43.
- Rubio, V., F. Linhares, R. Solano, A.C. Martín, J. Iglesias, A. Leyva and J. Paz-Ares. 2001. A conserved MYB transcription factor involved in phosphate starvation signaling both in vascular plants and in unicellular algae. *Genes & Develop.*, 15(16): 2122-2133.
- Shen, C.W., J. Wang, X.Q. Shi, Y.L. Kang, C.Y. Xie, L.R. Peng, C.X. Dong, Q.R. Shen and Y.C. Xu. 2017. Transcriptome analysis of differentially expressed genes induced by low and high potassium levels provides insight into fruit sugar metabolism of pear. *Front. Plant Sci.*, 8: 938.
- Shin, R., R.H. Berg and D.P. Schachtman. 2005. Reactive oxygen species and root hairs in Arabidopsis root response to nitrogen, phosphorus and potassium deficiency. *Plant Cell Physiol.*, 46: 1350-1357.
- Tian, X.L., G.W. Wang, R. Zhu, P.Z. Yang, L.S. Duan and Z.H. Li. 2008. Conditions and indicators for screening cotton (*Gossypium hirsutum*) genotypes tolerant to low-potassium. *Acta Agron Sin.*, 34(8): 1435-1443.
- Voelker, C., D. Schmidt, K. Czempinski and K. Czempinski. 2006. Members of the Arabidopsis AtTPK/KCO family form homomeric vacuolar channels in planta. *Plant J.*, 48(2): 296.
- Von, S.A. and S.A. Von. 2003. The oxidative pentose phosphate pathway: structure and organisation. *Curr. Opin. Plant Biol.*, 6(3): 236-246.
- Wang, R., W. Jing, L.Y. Xiao, Y.K. Jin, L.K. Shen and W.H. Zhang. 2015. The rice high-affinity potassium transporter1;1 is involved in salt tolerance and regulated by an MYB-type transcription factor. *Plant Physiol.*, 7(168): 1076-1090.
- Wang, S., Y. Bai, C. Shen, Y.R. Wu and S.N. Zhang. 2010. Auxin-related gene families in abiotic stress response in *Sorghum bicolor*. *Func. & Integ. Genom.*, 10(4): 533-546.
- Wang, Y., L. He, H.D. Li, J. Xu and W.H. Wu. 2010. Potassium channel α -subunit At KC1 negatively regulates AKT1-mediated K⁺ uptake in Arabidopsis roots under low-K⁺ stress. *Cell Res.*, 20: 826-837.
- Wang, Y.H., D.F. Garvin and L.V. Kochian. 2002. Rapid induction of regulatory and transporter genes in response to phosphorus, potassium, and iron deficiencies in tomato roots. Evidence for cross talk and root/rhizosphere-mediated signals. *Plant Physiol.*, 130(3): 1361-1370.
- Wang, Z.W., N. Hobson, L. Galindo, S.L. Zhu, D.H. Shi, J. McDill, L.F. Yang, S. Hawkins, G. Neutelings, R. Datla, G. Lambert, D.W. Galbraith, C.J. Grassa, A. Gerald, Q.C. Cronk, C. Cullis, P.K. Dash, P.A. Kumar, S. Cloutier, A.G. Sharpe, G.K. Wong, J. Wang and M.K. Deyholos. 2012. The genome of flax (*Linum usitatissimum*) assembled de novo from short shotgun sequence reads. *Plant J. Cell & Mol. Biol.*, 72(3): 461-473.

- Wu, J.T., X.Z. Zhang, T.X. Li, H.Y. Yu and P. Huang. 2011. Differences in the efficiency of potassium (K) uptake and use in barley varieties. *Agri. Sci. China*, 10(1): 101-108.
- Xu, J., H.D. Li, L.Q. Chen, Y. Wang and L.L. Liu. 2006. A protein kinase, interacting with two calcineurin B-like proteins, regulates K⁺ transporter AKT1 in Arabidopsis. *Cell*, 125(7): 1347-1360.
- Yang, X.E., J.X. Liu, W.M. Wang, H. Li, A.C. Luo, Z.Q. Ye and Y. Yang. 2003. Genotypic differences and some associated plant traits in potassium internal use efficiency of lowland rice (*Oryza sativa* L.). *Nutrient Cycling in Agroecosystems*, 67: 273-282.
- Yang, Z. M., Q.M. Li, B. Wang, S.D. Bao and R.H. Shi. 1998. Study on method for screening winter wheat genotypes tolerant to low potassium level. *Acta Pedol. Sin.*, 35: 376-383.
- Zeng, J.B., X.Y. He, D.Z. Wu, B. Zhu, S.G. Cai, U.A. Nadira, Z.H. Jabeen and G.P. Zhang. 2014. Comparative transcriptome profiling of two tibetan wild barley genotypes in responses to low potassium. *Plos One*, 9(6): 1371.
- Zeng, Q.Y., Q.P. Ling, L.N. Fan, Y. Li, F. Hu, J.W. Chen, Z.R. Huang, H.H. Deng, Q.W. Li and Y.W. Qi. 2015. Transcriptome profiling of sugarcane roots in response to low potassium stress. *Plos One*, 10(5): 1371.
- Zhang, X.Q., H. Jiang, H. Wang, J. Cui, J.H. Wang, J. Hu, L.B. Guo, Q. Qian and D.W. Xue. 2017. Transcriptome analysis of rice seedling roots in response to potassium deficiency. *Sci. Reports*, 7(1): 5523.
- Zhao, D.B., F.X. Zhang, F.Z. Guan, L. Ni, Q.B. Zhang and Y. Zhang. 1991. Study on the effect of potassium on the yield and quality of flax fiber. China. *Fiber Crops*, (2)21-22 (Chinese with English abstract).

(Received for publication 10 March 2018)